



## A model of cockpit karst landscape, Jamaica

Cyril Fleurant, G.E. Tucker, H.A. Viles

► **To cite this version:**

Cyril Fleurant, G.E. Tucker, H.A. Viles. A model of cockpit karst landscape, Jamaica. *Geomorphologie -Paris-*, Gfg, 2008, pp.3-14. <hal-00735525>

**HAL Id: hal-00735525**

**<https://hal.archives-ouvertes.fr/hal-00735525>**

Submitted on 25 Sep 2012

**HAL** is a multi-disciplinary open access archive for the deposit and dissemination of scientific research documents, whether they are published or not. The documents may come from teaching and research institutions in France or abroad, or from public or private research centers.

L'archive ouverte pluridisciplinaire **HAL**, est destinée au dépôt et à la diffusion de documents scientifiques de niveau recherche, publiés ou non, émanant des établissements d'enseignement et de recherche français ou étrangers, des laboratoires publics ou privés.

# A model of cockpit karst landscape, Jamaica

## Modélisation d'un paysage de karst de type cockpit (Jamaïque)

Cyril Fleurant\*, Gregory E. Tucker\*\*, Heather A. Viles\*\*\*

### Abstract

This paper deals with a landscape evolution model to compute cockpit karsts landforms. The CHILD model is used to model geomorphic processes at regional scale. After examining briefly CHILD's principles and equations of limestone dissolution processes, the denudation model is detailed. The relation between subcutaneous dissolution and denudation of the topography is introduced by means of an empirical equation associated with epikarst processes: the denudation is taken to be proportional to the dissolution in the subcutaneous zone. The model takes into account an anisotropic dissolution in space according to what is observed in reality or described by scenarios of cockpit karst landscape evolution. Simulated cockpit karst terrains are compared with real landscapes by means of several morphometric criteria: slope, relative relief and scaling properties. Results confirm the importance of anisotropic dissolution processes and could provide a numerical validation of the epikarst processes to describe cockpit karst genesis.

**Key words:** model, landscape evolution, karst denudation, subcutaneous zone, morphometric analysis.

### Résumé

Cet article présente une étude sur l'utilisation d'un modèle numérique morphogénétique développé afin de pouvoir simuler l'évolution de la forme des karsts en cockpits. Le modèle CHILD est ici utilisé pour une modélisation à petite échelle (paysage entier). Dans un premier temps, nous rappelons le fonctionnement de CHILD ainsi que les équations qui décrivent les processus de dissolution des carbonates. Puis, nous donnons les détails du modèle d'érosion, basé sur les principes de fonctionnement de l'épikarst : la relation entre la dissolution souterraine des carbonates et l'érosion en surface est introduite par le biais d'une relation empirique. Ainsi l'érosion est considérée comme proportionnelle à la dissolution de la zone sous-cutanée. Dans cette approche, le modèle prend en compte l'anisotropie spatiale conformément à ce qui est observé dans la réalité ou est encore décrit par des scénarios de l'évolution des karsts de type cockpit. Les paysages simulés sont comparés aux paysages réels grâce à des indices morphométriques : la pente, le relief relatif et les propriétés de variation d'échelle de la topographie. Les résultats confortent à la fois l'importance de la prise en compte de l'hétérogénéité spatiale de la dissolution et surtout la validité de la prise en compte de l'épikarst pour décrire la genèse des karsts de type cockpit.

**Mots clés :** modèle, évolution géomorphologique, cockpit, érosion karstique, zone sous-cutanée, analyse morphométrique.

### Version française abrégée

Les karsts de type cockpit sont présents dans certaines régions tropicales humides où les précipitations dépassent en moyenne 1 500 mm/an, lorsque les conditions lithologique peuvent favoriser leur développement. Ces paysages particuliers se présentent comme une succession de dépressions et de collines. Leur développement est comparable à celui des dolines (fig. 1). La modélisation des processus géomorphologiques est rendue possible depuis plusieurs dizaines d'années grâce à l'utilisation de simulations numériques de plus en plus performantes. Ces codes de calcul

permettent de simuler la non-linéarité et l'interaction des processus qui façonnent les formes du relief.

Dans une étude précédente, C. Fleurant et al. (2007) ont exposé une méthode de simulation pour un seul cockpit (0,01 km<sup>2</sup>). L'objectif de cet article est d'étudier les conditions topographique, hydrologique et géochimique nécessaires au développement des formes de karst de type cockpit pour un ensemble plus vaste (16 km<sup>2</sup>), mais du fait du très grand changement d'échelle spatiale des formes étudiées les processus géomorphologiques, ainsi que les équations utilisées, ne peuvent être simplement transposées. Les auteurs utilisent le modèle CHILD en y intégrant les processus liés

\* Département Paysage, Institut National d'Horticulture, 2 rue Le Notre, 49045 Angers Cedex 01, France. Courriel : cyril.fleurant@inh.fr

\*\* Department of Geological Sciences, Cooperative Institute for Research in Environmental Sciences, University of Colorado, Boulder, USA. E-mail: gtucker@cires.colorado.edu

\*\*\* Centre for the Environment, University of Oxford, South Parks Road, Oxford OX1 3QY, UK. E-mail: heather.viles@ouce.ox.ac.uk

à la dissolution chimique des carbonates. CHILD est un modèle numérique géomorphologique (Tucker et al., 1999) qui simule l'évolution des formes de la topographie dans le temps. Ces formes sont la résultante de l'interaction et d'un feed-back positif entre les écoulements, l'érosion et la sédimentation. Comme les processus de dissolution sont principalement à l'origine des formes de karst de type cockpit, l'évolution de la topographie peut se ramener à l'équation (2). CHILD fonctionne sur le principe d'une discrétisation spatio-temporelle (fig. 2 et équation 3) qui permet de résoudre les équations aux dérivées partielles suivant un schéma numérique explicite. L'évolution de la topographie est fondée sur une hypothèse expliquée par les principes de fonctionnement de l'épikarst : les écoulements souterrains et l'érosion chimique de surface peuvent être traduits mathématiquement par l'équation (7). Dans ce cas, l'érosion de la topographie est indirectement liée à la dissolution de la roche de la zone épikarstique (fig. 3).

La géométrie initiale adoptée pour la zone d'étude est une surface lisse et légèrement ondulée de 16 km<sup>2</sup> ( $X = Y = 4\ 000\ m$ ). L'altitude moyenne de ces ondulations est  $Z_0 = 600\ m$ . Ces ondulations représentent une succession de sommets ( $Z_0 + 10\ cm$ ) et de dépressions ( $Z_0 - 10\ cm$ ) (fig. 4) qui sont destinées à guider les écoulements de l'eau en début de simulation. Cette surface lisse et ondulée que nous pouvons assimiler à un plateau est discrétisée en 40 000 cellules de Voronoï. Chaque nœud, centré sur la cellule de Voronoï, est donc représentatif d'une zone de l'ordre de 400 m<sup>2</sup>.

L'objectif des simulations est de tester l'approche du modèle (équation 7) afin de savoir si les processus géomorphologiques mis en équation permettent de recréer les formes typiques des karsts de type cockpit. Pour cela nous avons comparé les paysages simulés (fig. 5) aux paysages réels grâce à trois indices morphométriques : la pente moyenne, le relief relatif (hauteur entre les dépressions et les sommets des cockpits) et les propriétés d'échelle du relief. P. Lyew-Ayee (2004) a montré que ces trois indices sont discriminants pour caractériser, dans la région des « cockpits country » de Jamaïque, les paysages de karst de type cockpit. Les paramètres des simulations sont présentés dans le tableau 1 et les données de terrain dans le tableau 2. Trois simulations ont été menées en faisant varier le facteur climatique (équation 4). Les simulations donnent des paysages numériques (fig. 5) qui sont analysés et comparés aux paysages réels par le biais d'indices morphométriques (fig. 6 à 11).

Les ressemblances entre les paysages morphologiques réels et ceux qui sont simulés constituent dans un premier temps une étape essentielle de notre étude, puisqu'elles valident la modélisation des processus. L'hypothèse de départ relative à l'influence de l'épikarst (processus souterrain de dissolution) sur la formation du karst de type cockpit (processus de surface) qui a été mise en équations dans le modèle semble être validée par les résultats. Ceux-ci montrent que pour simuler la genèse du karst de type cockpit ressemblant à celui que l'on observe dans les régions tropicales, la quantité des précipitations doit être au moins supérieure à 1,5 m/an, ce qui est parfaitement cohérent avec les études de

nombreux auteurs (e.g. Sweeting, 1972). À l'échelle des temps géologiques, le facteur climatique montre l'importance des précipitations. Il tend vers 1 lorsque la durée de la saison pluvieuse augmente. Les résultats des simulations montrent clairement l'impact fort de ce facteur climatique sur la morphologie des paysages de karst obtenus. Pour les valeurs des paramètres du modèle, nous pouvons conclure que les modèles du karst de type cockpit n'ont pu se former que pour des précipitations abondantes pendant une longue saison des pluies().

## Introduction

Landscape evolution is the result of various forces: tectonics, erosion, deposition, which in turn, are governed by complex processes related to lithospheric movements, climatic conditions and rock properties. A better understanding of landscape evolution can be assisted by numerical tools that make it possible to explore the complex non-linear and interacting processes shaping landscapes. Significant progress has been made in quantifying the evolution of drainage-basin landscapes by physical processes such as mechanical weathering, sediment transport on hillslopes and channels, and channel incision into bedrock. For many of these processes, we now have geomorphic transport laws that describe their long-term impact on topography (see review by Dietrich *et al.*, 2003). In contrast, few quantitative models exist to describe chemical geomorphic processes and their role in shaping karst terrain. In this paper, we study the evolution of cockpit karst landscapes by means of a simulation model.

Karst is terrain that possesses distinctive hydrology and landforms as a result of high rock solubility and well-developed secondary porosity (Ford and Williams, 1989). Often, but not always, found in areas underlain by carbonate rocks such as limestone and dolomite, karst terrain appears very distinct to 'normal' fluvial landscapes with a lack of established surface drainage networks. Major surface karst landforms include enclosed depressions such as dolines, which are the major routeways by which water is translated from the surface to the subsurface zone. Several conceptual models of karst landscapes stress the importance of the epikarstic zone (i.e. the uppermost zone of weathered bedrock below the soil) which is usually heavily fissured and is the location for most dissolutional activity (Williams, 1983). In the past, a clear climatic control on karst landscapes was recognised, and although a simplistic link between climate and relief is now less accepted, temperate karst areas are often characterised by polygonal networks of dolines whilst humid tropical karsts often consist of networks of dramatic hills. In Jamaica and other areas, conical hills are separated by deep dolines (called cockpits) making up what is known as 'cockpit karst' (fig. 1).

Over the last ten years, much effort has been focused on developing models that can simulate landscape evolution on large time and space scales (e.g. Willgoose *et al.*, 1991; Braun and Sambridge, 1997; Tucker *et al.*, 2001). Most such models incorporate both short-range processes such as hill slope diffusion, and long-range processes such as fluvial

Fig. 1 – An oblique aerial view of cockpit karst terrains in Jamaica (Photo by P. Lyew-Ayee).

Fig. 1 – *Vue aérienne oblique d'un paysage de karst en cockpits dans la région de « Cockpit Country » en Jamaïque* (photo de P. Lyew-Ayee).



transport. A partial list of current models includes SIBERIA (Willgoose *et al.*, 1991), GOLEM (Tucker and Slingerland, 1994), DELIM (Howard, 1994), CASCADE (Braun et Sambridge, 1997), CAESAR (Coulthard *et al.*, 1998), ZSCAPE (Densmore *et al.*, 1998), and CHILD (Tucker *et al.*, 1999) and they are reviewed in Coulthard (2001).

Although modelling of subsurface runoff and relief generation in karst has resulted in considerable research (Groves and Howard, 1994; Clemens *et al.*, 1997; Kaufman and Braun, 1999, 2000), very few models explore rock dissolution processes by surface water and surficial landscape evolution (Ahnert and Williams, 1997; Kaufman and Braun, 2001).

Starting from a squared two-dimensional network and simple erosion laws, Ahnert and Williams (1997) recreated tower karst landscapes. Kaufman and Braun (2001) demonstrated how carbon dioxide-enriched surface runoff shapes a landscape typical of large karstic valleys by the chemical dissolution of calcite contained in rocks. They used the CASCADE model for their study, and included an erosion factor related to the dissolution of carbonate rocks. Fleurant *et al.* (2007) used the CHILD model to simulate the evolution on a single cockpit.

A wide variety of karst landscapes exist whose morphologies depend on a number of variables (White, 1984): chemical variables such as temperature, pressure of carbon dioxide and rainfall; physical variables such as relief and rainfall; geological variables such as tectonics, characteristic features of soluble rocks, stratigraphy and lithology. The variations of the different components listed above over a range of timescales result in different landscapes: doline karst, fluvio-karst or tower karst. Nevertheless, a common characteristic of karst landscapes is that they are mainly composed of a series of closed depressions and hills (Trudgill, 1985).

Cockpit karst is a form of polygonal karst usually thought to occur only under humid tropical climatic conditions. Polygonal karst (Ford and Williams, 1989) is characterised by a network of closed depressions covering an entire landscape; cockpit karst is a variant of this where the closed depressions are deep, large and often star-shaped with residual hills found between them. In order for cockpit karst to form several requirements must be met, i.e. abundant runoff, massive and pure limestones, and a regional system of fractures which allow the development of underground drainage

(White, 1984). Sweeting (1972) hypothesizes that annual rainfall of over 1500 mm is required to form cockpit karst. The type site for cockpit karst is found in the Cockpit Country in Jamaica, where the landscape is underlain by White Limestone, a massive and exceptionally pure unit (Lyew-Ayee, 2004). Karstic processes are characterised by the predominance of mass transport of solutes over other transport processes (White, 1984). This is why the integration of carbonate rock dissolution processes is essential for the modelling karstic phenomena.

The objective of the present paper is to examine the topographic, hydrologic, and geochemical conditions under which cockpit karst can develop. We describe the integration of chemical dissolution processes of carbonate rocks in the computer model CHILD. Integrating chemical erosion into the model will allow us to test some hypotheses of cockpit karst landscape development in Jamaica, and will also permit further testing of karst landscape evolution theories.

We will consider briefly the functioning principles of the CHILD model as well as the modifications which were necessary to simulate rock dissolution processes. These modifications build upon the work presented in Fleurant *et al.* (2007) and are now tested at the regional scale. The simulated landscape will be compared to a real cockpit karst landscape through three morphometric criteria typical of this type of landscape, and recently highlighted by Lyew-Ayee (2004): average slope, relative relief and scaling characteristics. Such a comparison will make it possible to provide both ranges of validity for the various parameters of dissolution models and put forward hypotheses of scenarios for cockpit formation.

## Geomorphological model

The CHILD model (Channel-Hillslope Integrated Landscape Development) is a numerical model of landscape evo-

lution (Tucker *et al.*, 1999). The evolution of topography over time is simulated through the interaction and feedback between surface flows, rock erosion and the transport of sediments. CHILD is a numerical simulation method used for modelling a large number of processes related to the geomorphology of catchment basins. As it has been well-described in previous work, we will consequently only present a small number of these features. In this computer model, the evolution of topography over time results from the combination of several factors:

$$\frac{dz_i}{dt} = \frac{dz_i}{dt}\Big|_{\text{diffusion}} + \frac{dz_i}{dt}\Big|_{\text{erosion}} + \frac{dz_i}{dt}\Big|_{\text{tectonic}} + \frac{dz_i}{dt}\Big|_{\text{dissolution}} \quad (1)$$

These various factors are numerically solved using a particular spatial framework: Voronoï polygons. The first three factors are present in most models of landscape evolution; a detailed description can be found in Tucker *et al.* (2001). The last factor, concerning rock dissolution, will be discussed in a subsequent section. Here we focus on dissolution processes of limestone, the other processes are neglected. Several studies (e.g. White, 1984 or Lyew-Ayee, 2004) and the presence of thick equatorial forest strengthen the assumption of the dissolution erosion predominance over mechanical erosion. So equation (1) reduces to:

$$\frac{dz_i}{dt} = \frac{dz_i}{dt}\Big|_{\text{dissolution}} \quad (2)$$

Implications of uplift and mechanical erosion are discussed in several papers (e.g. Pfeffer, 1997). Cockpit karst landforms in Jamaica are restricted to areas of the White Limestone Group. This white limestone was first exposed to erosion by uplift in the Upper Miocene and no traces can be discerned today of a surface drainage system in the cockpit areas. Thus, we assume that landscape development from the Miocene onwards has been dominated by solutional processes, without any significant contribution from either other denudation processes or tectonics.

## Spatial discretization

The spatial framework of the CHILD model is composed of an irregular network of points and is used to obtain a reliable discretization of the topographic surface. These points, also called nodes, are connected to form a mesh of triangles known as a Triangulated Irregular Network, or TIN (Braun and Sambridge, 1997; Tucker *et al.*, 2001). This gridded model is built up using Delaunay triangulation and offers several advantages over a raster-based approach (Braun and Sambridge, 1997; Tucker *et al.*, 2001). From the numerical point of view, triangulation makes it possible to solve equations involving partial derivatives using the finite-volume method (Versteeg and Malalasekera, 1995). Each node of the triangulation is associated with a Voronoï cell (fig. 2). Such a method can thus be used to solve physical equations related to geomorphologic processes, with exchanges of mass between nodes calculated at the Voronoï polygon interfaces.

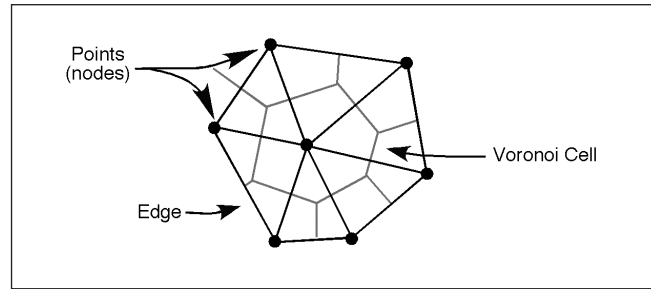


Fig. 2 – Schematic illustration of the spatial framework in CHILD model. The study area (16 km<sup>2</sup>) is discretized into 40000 Voronoï cells. Each cell is 400 m<sup>2</sup> large.

Fig. 2 – Illustration schématique du mode de discrétisation du modèle CHILD. La zone d'étude a une surface de 16 km<sup>2</sup> et est découpée en 40 000 cellules de Voronoï. Chaque cellule de Voronoï représente une surface de 400 m<sup>2</sup>.

## Temporal discretization

The temporal framework of the CHILD model makes it possible to consider the significant time disparities resulting from geomorphologic processes: the evolution of topography spreads over thousands of years, whereas rainfall frequency can range from a few minutes to a few days. Rainfall variability at a geological time scale is simulated using a stochastic method based on a Poisson storm-arrival model and exponentially distributed storm intensity and duration, which gives the distribution of rainfall frequency and intensity (Tucker and Bras, 2000). Equations are solved iteratively, according to an alternation of rainy and dry periods. Storm intensity and duration are assumed to be independent. The probability density functions for storm intensity, duration and interstorm interval are given by:

$$\begin{aligned} fdp(P) &= \frac{1}{P} \exp\left(-\frac{P}{P}\right) \\ fdp(T_r) &= \frac{1}{T_r} \exp\left(-\frac{T_r}{T_r}\right) \\ fdp(T_b) &= \frac{1}{T_b} \exp\left(-\frac{T_b}{T_b}\right) \end{aligned} \quad (3)$$

The mean annual rainfall  $\langle P \rangle$  is linked with  $\bar{P}$ :

$$\langle P \rangle = \bar{P} \frac{\bar{T}_r}{\bar{T}_r + \bar{T}_b} \quad (4)$$

The parameter  $\frac{\bar{P}}{\langle P \rangle}$

can be thought of as a climate variability factor (Tucker and Bras, 2000).

Surface runoff is modelled using an algorithm that routes water from one cell to the next following the path of steepest descent. In the case of an enclosed depression, water either evaporates or is forced to find an outlet, using a lake-filling algorithm (Tucker *et al.*, 2001). Local runoff generation, at one node, can be modelled using several functions: Horton runoff or excess runoff on saturated soils.

## Calcite dissolution and karst denudation

Although calcite is slightly soluble in deionised water, most karst denudation occurs through the dissolution of calcite by water acidified by carbon dioxide. In the case of open systems, carbonates are affected by climatic events (rain in the studied case) and other flowing waters (rivers for example). The dissolution of carbonate rocks will then depend on the flux of water in contact with carbonates, and on the hydrodynamic nature of flows (Dreybrodt, 1988).

The calcite dissolution process in an open system can then be expressed as follows (Trudgill, 1985):



It should be noted that, for stoichiometric reasons, one mole of  $\text{Ca}^{2+}$  consumes one mole of  $\text{CO}_2$ . Consequently, the absolute flow value of  $\text{CO}_2$  is equal to that of  $\text{Ca}^{2+}$ .

The karst denudation process corresponds to the erosion of carbonates through dissolution. Several models have been put forward to quantify this erosion (Corbel, 1959; Ford, 1981). White's (1984) denudation model ( $DR$ ) is the most comprehensive and widely used; it speculates that infiltration waters and carbonates are in equilibrium:

$$DR = -1000 \frac{m_{\text{Ca}}}{\rho_{\text{CaCO}_3}} < P > \left( \frac{K_1 K_C K_H P_{\text{CO}_2}}{4 K_2 \gamma_{\text{Ca}} \gamma_{\text{HCO}_3}^2} \right)^{\frac{1}{3}} \quad (5)$$

where  $K_1$  ( $\text{mol}/\text{m}^3$ ),  $K_2$  ( $\text{mol}/\text{m}^3$ ),  $K_C$  ( $\text{mol}^2/\text{m}^6$ ) and  $K_H$  ( $\text{mol}/\text{m}^3/\text{atm}$ ) are equilibrium constants which only depend on temperature,  $\gamma_X$  is the activity coefficient of  $X$  and  $P_{\text{CO}_2}$  (atm.) is the pressure of carbon dioxide in open system, *i.e.* under atmospheric conditions. The  $DR$  values may vary according to the temperature and  $\text{CO}_2$  pressure. The values of  $P_{\text{CO}_2}$  pressure depend on local factors: the atmospheric conditions and soil biological activity. The relation between  $P_{\text{CO}_2}$  and the actual evapotranspiration rate ( $E$ ) and therefore the geographical variation of carbon dioxide pressure in soils is (Brook and Hanson, 1991):

$$\log(P_{\text{CO}_2}) = -3.47 + 2.09(1 - e^{-0.00172 < E >}) \quad (6)$$

In Jamaica for example,  $E \approx 1$  m/y, which gives  $P_{\text{CO}_2} \approx 0.0176$  atm. Such values are consistent with the values Smith *et al.* (1976) put forward for tropical areas:  $P_{\text{CO}_2} \approx 0.01$  atm.

The relation (5) combines rock, equilibria and climatic factors. Each of the three climatic variables (temperature, carbon dioxide pressure and effective rainfall) has a different impact on denudation rate. In order of importance, the key controls are: effective rainfall (linear relation), carbon dioxide pressure (cube root relation) and temperature, which has a non-linear influence on chemical constants. As mentioned previously, White's model (1984) gives the maximum value of karst denudation for the whole studied area. Therefore, if the model (5) is applied, it is assumed that the karst denudation rate is uniform across the studied

karst. For typical values of cockpit karst terrains  $DR \approx 130$  mm/ky (Smith *et al.*, 1976).

## Model concepts

As the karstification process is complex it is difficult to establish clear and quantifiable relations between its various components: calcite dissolution, geologic properties of carbonates, rock structure, and climatic variations. There is a considerable literature on the qualitative description of these processes (e.g. Jennings, 1985; Sweeting, 1972; Williams, 1985), but little modelling work has so far been produced quantifying these. Although dissolution plays an essential role in the development of karst, it is not the only process involved with collapse, and subsidence brings material down into closed depressions (Jennings, 1985). Many authors also highlight the close relation between surface denudation and underground karstification processes, but do not provide quantitative data to link the two (Dreybrodt, 1988).

These linkages are strongly suggested by the epikarst zone (e.g. Ford and Williams, 1989). The epikarst is the uppermost zone of highly weathered karst bedrock below the soil. Runoff waters passing through the soil become enriched in carbon dioxide, producing a maximum dissolution rate within the epikarst zone. Most dissolution is accomplished within 10 m of the surface as a result. This dissolution within the epikarst zone leads directly to surface lowering, as soils subside into the enlarged voids created. Thus, the higher the subsurface dissolution rate, the more rapidly topography lowers over time. Therefore, in the model presented in this paper, the rate of dissolution of topography is taken to be proportional to the underground dissolution.

## The mathematical model

Equations of the model express a simple linear relationship between surface denudation rate and underground dissolution, thus subsurface flow:

$$\frac{\partial z_i}{\partial t} \Big|_{\text{dissolution}} = - \left[ \frac{DR_{\text{max}} - DR_{\text{min}}}{q_{\text{max}} - q_{\text{min}}} (q_i - q_{\text{max}}) + DR_{\text{max}} \right] \quad (7)$$

where  $z_i$  (m) is the altitude of the node  $i$ ,  $DR_{\text{max}}$  (m/s) and  $DR_{\text{min}}$  (m/s) are respectively the maximum and the minimum denudation rates on the study area,  $q_i$  ( $\text{m}^3/\text{s}$ ) is the subsurface flow going through the Voronoï cell  $i$ ,  $q_{\text{max}}$  ( $\text{m}^3/\text{s}$ ) and  $q_{\text{min}}$  ( $\text{m}^3/\text{s}$ ) are respectively the maximum and the minimum subsurface flow on the study area at time  $t$  (s). Equation (7) is illustrated by figure 3: the more subsurface flow increases, the more denudation rate increases.

## Boundary and initial conditions

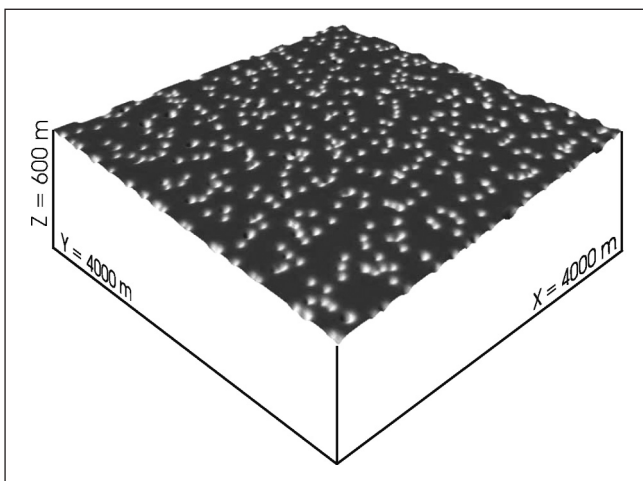
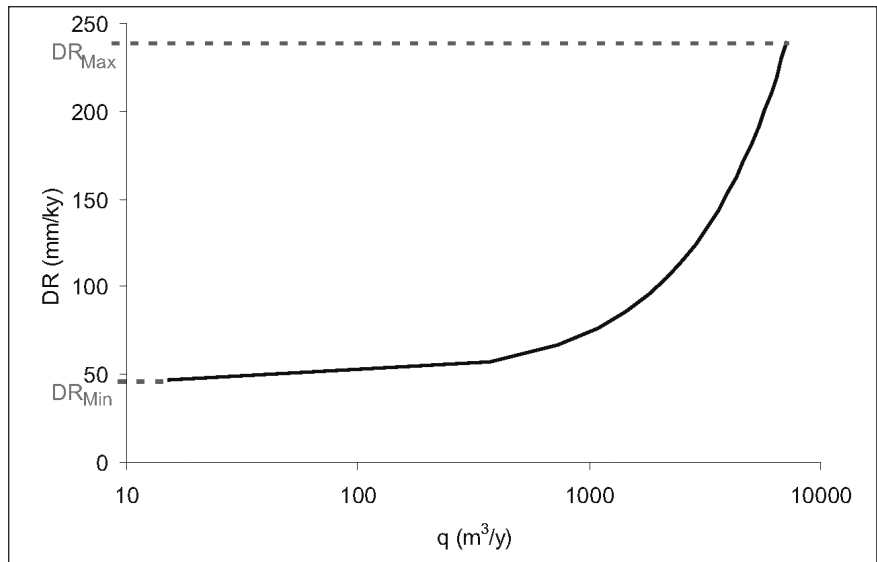
It is assumed that development of cockpit landforms begins on a smooth gently undulating surface ( $X = Y = 4000$  m). The average altitude of these depressions and summits is  $Z_0 = 600$  m (fig. 4). In fact, following the

Fig. 3 – **Principle of equation (7).** Denudation rate of the topography DR is taken to be proportional to the underground flow q (subcutaneous zone).

Fig. 3 – **Illustration du fonctionnement de l'équation (7).** L'érosion karstique DR est directement en relation avec le flux de subsurface q (zone épikarstique).

Fig. 4 – **Boundary conditions.** Initial topography is a smooth 600 m high surface with random sinks (-10 cm). The density of these depressions is 25 km<sup>2</sup>.

Fig. 4 – **Conditions aux limites.** La topographie initiale est une surface lisse de 600 m d'altitude sur laquelle sont réparties aléatoirement des dépressions (-10 cm). La densité de ces dépressions est d'une pour 25 km<sup>2</sup>.



of each Voronoï cell is 10<sup>-7</sup> m/s. This value is typical of slow initial karstification processes (Singhal and Gupta, 1999). This hydraulic conductivity controls the partitioning of surface runoff and subsurface flow. Initially, depressions, cockpits or sinks are created using a random uniform function in the study area (16 km<sup>2</sup>). The density of sinks is approximately  $d = 25 \text{ km}^{-2}$  (fig. 5). This average value was calculated by Lyew-Ayee (2004) for the whole cockpit country in Jamaica. In the model, the value of rainfall is  $\langle P \rangle = 2 \text{ m/y}$ . Many field studies (e.g. Sweeting, 1972) clearly show that average rainfall has to be greater than 1 m/yr to produce cockpit karst landscapes. Moreover, actual average effective rainfall in Jamaica is about 2 m/yr (Lyew-Ayee, 2004).

The local maximum and minimum denudation rates were estimated by Smith *et al.* (1972) in the Cockpit karst areas:

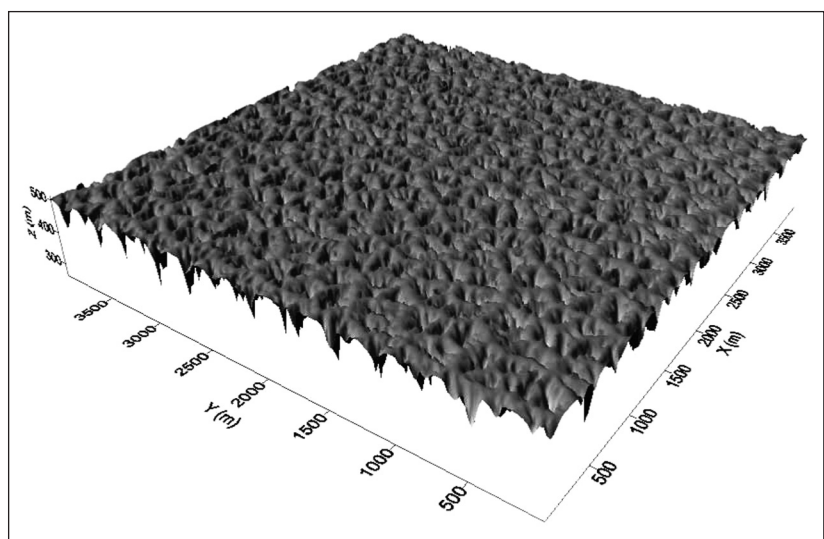
$$\begin{aligned} DR_{\min} &= (CaCO_3)_{\min} \frac{\langle P \rangle}{\rho_{CaCO_3}} \\ DR_{\max} &= (CaCO_3)_{\max} \frac{\langle P \rangle}{\rho_{CaCO_3}} \end{aligned} \quad (8)$$

limestone sediment deposition that occurred during the Oligocene and Eocene, the cockpit area of Jamaica is thought to have undergone a tectonic elevation of the ground, from subaqueous to approximately  $Z_0 = 600 \text{ m}$  above sea level (Lyew-Ayee, 2004). Consequently, the karstification process is presumed to have only started during the Pliocene, when climatic conditions were favourable (Pfeffer, 1997).

The limestone plateau is discretized into 40000 Voronoï cells. Hydraulic conductivity

Fig. 5 – **Example of a simulated cockpit karst landscape.** Here, the climatic factor is 2 and the simulation time is 4 My. The DEM of a simulated landscape can be used to perform analysis. In this study, three analyses are carried out: average slope, relative relief and scaling characteristics.

Fig. 5 – **Exemple d'un paysage de karst en cockpit simulé.** Pour cette simulation, le facteur climatique est de 2 et le temps de simulation est de quatre millions d'années. Le MNT simulé, peut ainsi être analysé : calculs de la pente moyenne, du relief relatif moyen, des propriétés d'échelle.



where  $(CaCO_3)$  (ppm) is the minimum or maximum hardness values of  $CaCO_3$  which were founded in the cockpit karst areas and  $r_{CaCO_3}$  ( $kg/m^3$ ) is volumetric weight of calcite. For values of the parameters given in the table 1, one obtains  $DR_{min} = 48$  mm/ky and  $DR_{max} = 240$  mm/ky. These denudation rates are local values of the limestone dissolution.  $DR_{min}$  occurs when subsurface flow is low whilst  $DR_{max}$  holds at higher values of subsurface flow. The average value of these denudation rates is 144 mm/ky which is very close to the typical value uses for cockpit karst terrains ( $DR = 130$  mm/ky from Smith *et al.*,1976).

## Results

The objective of simulations is to test the mathematical model (7), in order to assess its capacity to recreate geomorphologic processes typical of cockpit karst landscapes of the cockpit type.

## Field data

There has been considerable research effort expended on morphometric analysis of karst landscapes aiming at producing quantitative data with which to test landscape evolution models (e.g. Brook and Hanson, 1991). Such research has been vastly aided by the advent of digital datasets from which DEMs can be produced. Lyew-Ayee (2004) used a suite of morphometric techniques to characterise and analyse and area covering 84 km<sup>2</sup> of the cockpit karst in Jamaica. He proposed several parameters, which could be used to distinguish cockpit karst from other relief types, of which we use the following: average slope, relative relief and scaling properties. Slopes are calculated from the DEM using a moving window – a 3x3 cell kernel – which is displaced throughout the grid. To calculate slopes, a third-order finite difference estimator is used that is based on the eight outer points of the moving window. Determination of relative relief needs to identify sinks and summits within the landscape. Then relative relief may be determined using sink and summit points. A cluster analysis of both the average slope and the average relative relief, that is the distance between depressions and summits of cockpits, was used (Lyew-Ayee, 2004) as a crucial measure in distinguishing cockpit and non-cockpit karst landscapes. The scaling properties give a picture of the scale of variations of the horizontal and vertical characteristics of the landscape (Weissel *et al.*, 1994). These scaling properties can be studied by conducting neighbourhood analysis of the grid. The range of elevation within a specified horizontal radius (from 10 m to 4000 m) is calculated. Results of the scaling characteristics are plotted as a log-log plot. Data show a major scaling break in the plot of vertical relief versus horizontal scale at around 100 m in the X axis. This value reveal the average spacing between sinks and summits which is significant with those observe in initial geometry conditions of the model (fig. 6). Then, data clearly show two scales to the landscape: before and after the scaling break. Data can thus be fitted by a linear equation before and after this breaking scale:  $z = c(x,y)^m$  where  $c$  is an amplitude factor and  $m$  is a scaling exponent (tab. 2).

Parameters	Description	Unity	Value
<b>Geometry</b>			
X	Length: X direction	m	4000
Y	Width: Y direction	m	4000
Z <sub>0</sub>	Initial high of the topography	m	600
N	Number of Voronoï cells		40000
d	Density of sinks	km-2	25
<b>Climatic factors, geological-lithological characteristics</b>			
<P>	Precipitation	m/an	2
T <sub>r</sub>	Storm duration	y	100 à 1000
T <sub>b</sub>	Interstorm period	y	0 à 900
ρ <sub>CaCO3</sub>	Volumetrie weight of calcite	kg/m3	2400
(CaCO3) <sub>min</sub>	Minimum hardness of calcite	ppm	58
(CaCO3) <sub>max</sub>	Maximum hardness of calcite	ppm	282
DR <sub>min</sub>	Minimum denudation rate	mm/ky	48
DR <sub>max</sub>	Maximum denudation rate	mm/ky	240

Table 1 – Values of the model's parameters.

Tableau 1 – Description et valeur des paramètres utilisés pour les simulations du modèle.

Name of the 'Cockpit Country' area	Slope (en°)	Relatif relief (en m)	c (before x = 100 m)	c (after x = 100 m)	m (before x = 100 m)	m (after x = 100 m)
Barbecue bottom	31	74	0.08	11.21	1.45	0.44
Quickstep	24	54	0.099	9.01	1.33	0.45
Windsor	26	57	0.097	9.77	1.32	0.41

Table 2 – Morphometric properties of the Cockpit Country study area (Lyew-Ayee, 2004).

Tableau 2 – Propriétés morphométriques des trois zones d'étude dans la région des « Cockpit Country » (Lyew-Ayee, 2004).

## Model simulations

Starting from these boundary and initial conditions, and applying the model (7), is it possible to simulate the landforms of a cockpit karst at regional scale?

The model needs the input of many variable values (tab. 1) most of which are drawn from published sources



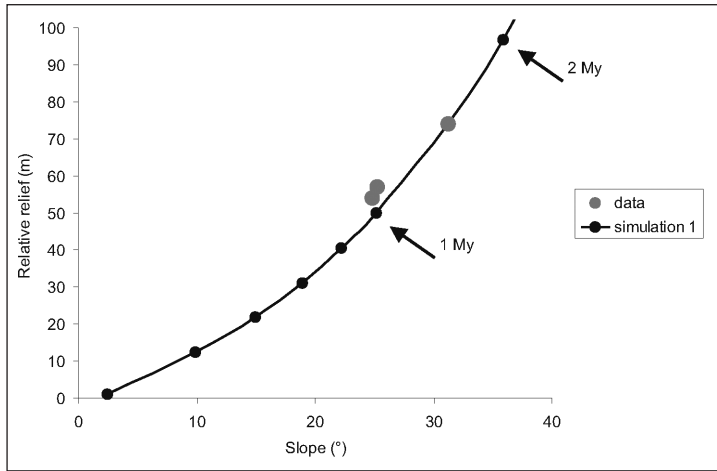


Fig. 6 – Evolution of average slope versus relative relief. The simulation 1 is computed with

$$\frac{\overline{T_r} + \overline{T_b}}{\overline{T_r}} = 1 \quad (\overline{T_r} = 1000 \text{ y and } \overline{T_b} = 0 \text{ y}).$$

Fig. 6 – Évolution de la pente moyenne en fonction du relief relatif moyen du paysage simulé. La simulation 1 correspond à un facteur climatique de

$$\frac{\overline{T_r} + \overline{T_b}}{\overline{T_r}} = 1 \quad (\overline{T_r} = 1000 \text{ ans et } \overline{T_b} = 0 \text{ an}).$$

(e.g. Smith *et al.*, 1972 or Lyew-Ayee, 2004). The only parameters which can be modified are the storm duration  $T_r$  and the interstorm period  $T_b$ . The duration ratio

$$\frac{\overline{T_r} + \overline{T_b}}{\overline{T_r}}$$

can be thought of as an intermittency factor or a climate variability factor (Tucker and Bras, 2000). In the present simulations, we change the value of the ratio from 1 to 10 to explore a large range of climate scenarios, where increasing the ratio will increase the intermittency of rainfall. Using the parameter values given in table 1, three simulations were carried out with different values for the climatic factor

$$\frac{\overline{T_r} + \overline{T_b}}{\overline{T_r}}$$

Simulations were run over a time period of 10 million years, based on published suggestions that karstification has been active here since the Pliocene (Pfeffer, 1997). The average hillslope and relative relief of the test-cockpit are computed every 10,000 years in order to note its evolution over time. Therefore, it is possible to compare the simulated values with the real average measurements of the test-cockpit in the studied area of Jamaica. The simulated landscapes (figure 5 is an example for

$$\frac{\overline{T_r} + \overline{T_b}}{\overline{T_r}} = 2 \text{ at } t = 4\text{My}$$

have been analysed in the same way as a DEM of a real cockpit karst landscape, with data collected for average slope, relative relief and scaling properties.

The results of the model simulations are shown in figures 6 to 9. Firstly, we can observe that the relative relief, the average slope and the scaling characteristics of the simulated landscape are quite similar to those observed in the field. These simulations lead to a key conclusion: using the chosen values of the model parameters, it is possible to recreate the morphometry of a cockpit karst landscape.

### Slope *versus* relative relief

The results presented in figures 6, 7 and 8 on the evolution of slope and relative relief show that changing the climatic factor does not change the resultant landforms but only the time interval required to produce them. If the climatic factor is

$$\frac{\overline{T_r} + \overline{T_b}}{\overline{T_r}}$$

the time needed to develop the same slope/relative relief value is

$$\frac{\overline{T_r} + \overline{T_b}}{\overline{T_r}} \text{ My.}$$

Therefore, the more the interstorm period increases, the longer the landscape takes to develop. Moreover, if one uses the slope/relative relief index to characterise the quality of the simulated landscape, the simulation is close to the real landscape when  $1 \text{ My} \leq t \leq 1.5 \text{ My}$  for

$$\frac{\overline{T_r} + \overline{T_b}}{\overline{T_r}} = 1 \text{ (fig. 6),}$$

when  $2 \text{ My} \leq t \leq 3 \text{ My}$  for

$$\frac{\overline{T_r} + \overline{T_b}}{\overline{T_r}} = 2 \text{ (fig. 7),}$$

and  $t > 10 \text{ My}$  when

$$\frac{\overline{T_r} + \overline{T_b}}{\overline{T_r}} = 10 \text{ (fig. 8).}$$

So, according to known information on the length of time available for cockpit karst formation in Jamaica (e.g. Pfeffer, 1997), the climatic factor used by the model must be less than 10, which is equivalent to having total storm duration at least nine times greater than interstorm periods:

$$\frac{\overline{T_r} + \overline{T_b}}{\overline{T_r}} < 10 \Rightarrow \overline{T_b} < 9\overline{T_r} \quad (9)$$

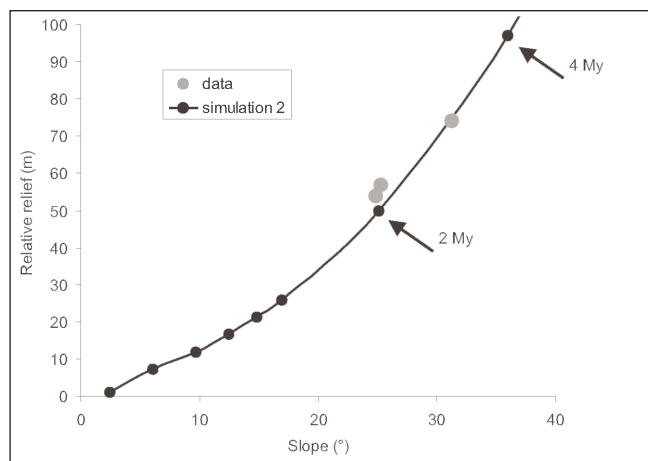


Fig. 7 – Evolution of average slope versus relative relief. The simulation 2 is computed with

$$\frac{\overline{T}_r + \overline{T}_b}{\overline{T}_r} = 2 \quad (\overline{T}_r = 500 \text{ y and } \overline{T}_b = 500 \text{ y}).$$

Fig. 7 – Évolution de la pente moyenne en fonction du relief relatif moyen du paysage simulé. La simulation 2 correspond à un facteur climatique de

$$\frac{\overline{T}_r + \overline{T}_b}{\overline{T}_r} = 2 \quad (\overline{T}_r = 500 \text{ ans et } \overline{T}_b = 500 \text{ ans}).$$

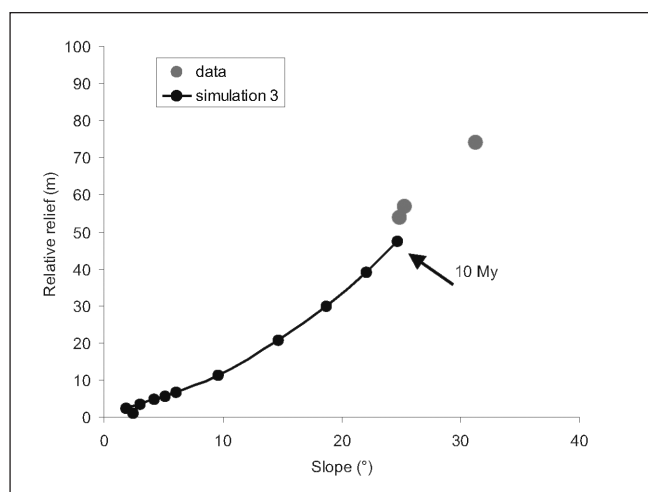


Fig. 8 – Evolution of average slope versus relative relief. The simulation 3 is computed with

$$\frac{\overline{T}_r + \overline{T}_b}{\overline{T}_r} = 10 \quad (\overline{T}_r = 100 \text{ y and } \overline{T}_b = 900 \text{ y}).$$

Fig. 8 – Évolution de la pente moyenne en fonction du relief relatif moyen du paysage simulé. La simulation 1 correspond à un facteur climatique de

$$\frac{\overline{T}_r + \overline{T}_b}{\overline{T}_r} = 10 \quad (\overline{T}_r = 100 \text{ ans et } \overline{T}_b = 900 \text{ ans}).$$

This result is very consistent with many authors' observations (e.g. Sweeting, 1972) that humid tropical climates, characterised by year-round abundant rainfall, are needed to produce a cockpit karst landscape.

## Scaling characteristics

Results of the scaling analysis are presented on figure 9. For each simulation, only three scaling curves are plotted corresponding to the most relevant times. Field data from the Jamaican cockpit karst clearly show a scaling break at around 100 m (average distance between sinks and summits), whereas these two scales (before and after 100 m) are less distinct within the simulated landscapes. The reason is probably due to the standard deviation of the average distance between sinks and summits. In the simulations, this distance is about 109 m, and the standard deviation is large (40 m), so that most of the distances range between 40 m and 180 m when the range of the distance in the field is from 80 m to 120 m only (Lyew-Ayee, 2004).

Concerning the scale less than 100 m, one can notice that simulations begin only at 20 m on the horizontal scale which is the grid resolution of the model. The scaling characteristics of the simulated landscapes, before and after the scaling break, show a relatively good general trend. But, if we go into the details one can notice (fig. 10) that relative (%) and absolute (m) errors are lower after the scaling break. This is probably due to the size of the model grid: the size of the Voronoï cells is, in average, 20 m. As the average radius of a cockpit is 109 m, we only have 5 Voronoï cells to model the hillslope landform of a cockpit. Beyond the horizontal scale  $(X,Y) = 100$  m, the landscape is analysed at a regional scale, so the grid size of the model (20 m) becomes less important.

The behaviour of the scaling characteristics curves *versus* the climatic factor is the same as that of the slope/relative relief index. Increasing the climatic factor, increases the time needed to obtain a landscape with similar landforms.

## Discussion and conclusion

Simulations carried out in the model are compared to real cockpit karst landforms from the Cockpit Karst Country in Jamaica. Morphometric characteristics can be deduced from simulated karst and compared with those measured from DEMs of real karst landscapes. Three morphologic characteristics based on Lyew-Ayee' work (2004) were chosen to compare simulated and real karst: average slope, relative relief and scaling characteristics.

The similarity between the simulated and real karst morphology constitutes an essential stage in the validation of the hypotheses put forward on their genesis. Though it is a necessary stage, it is probably not a sufficient one, and further tests need to be carried out to test the validity of our model. The present study highlights how essential it is to take spatial anisotropy of denudation into account when studying the morphometric evolution of cockpit karst.

The spatial anisotropy of denudation corresponds to the heterogeneity of many variables, e.g. hydraulic conductivity or depth of soil, which are frequently observed in karstic systems and that we have encapsulated in a simple linear model. Further work could usefully be done in the field in quanti-

Fig. 9 – **Scaling properties of the simulated landscape.** These virtual landscapes are simulated for several climatic factors:

$$(A) \frac{\overline{T}_r + \overline{T}_b}{\overline{T}_r} = 1 \quad (\overline{T}_r = 1000 \text{ y and } \overline{T}_b = 0 \text{ y}),$$

$$(B) \frac{\overline{T}_r + \overline{T}_b}{\overline{T}_r} = 2 \quad (\overline{T}_r = 500 \text{ y and } \overline{T}_b = 500 \text{ y})$$

$$\text{and (C) } \frac{\overline{T}_r + \overline{T}_b}{\overline{T}_r} = 10 \quad (\overline{T}_r = 100 \text{ y and } \overline{T}_b = 900 \text{ y}).$$

Fig. 9 – **Les propriétés d'échelle des paysages simulés.** Ces paysages virtuels sont simulés pour différentes valeurs du facteur climatique :

$$(A) \frac{\overline{T}_r + \overline{T}_b}{\overline{T}_r} = 1 \quad (\overline{T}_r = 1000 \text{ ans et } \overline{T}_b = 0 \text{ an}),$$

$$(B) \frac{\overline{T}_r + \overline{T}_b}{\overline{T}_r} = 2 \quad (\overline{T}_r = 500 \text{ ans et } \overline{T}_b = 500 \text{ ans})$$

$$\text{et (C) } \frac{\overline{T}_r + \overline{T}_b}{\overline{T}_r} = 10 \quad (\overline{T}_r = 100 \text{ ans et } \overline{T}_b = 900 \text{ ans}).$$

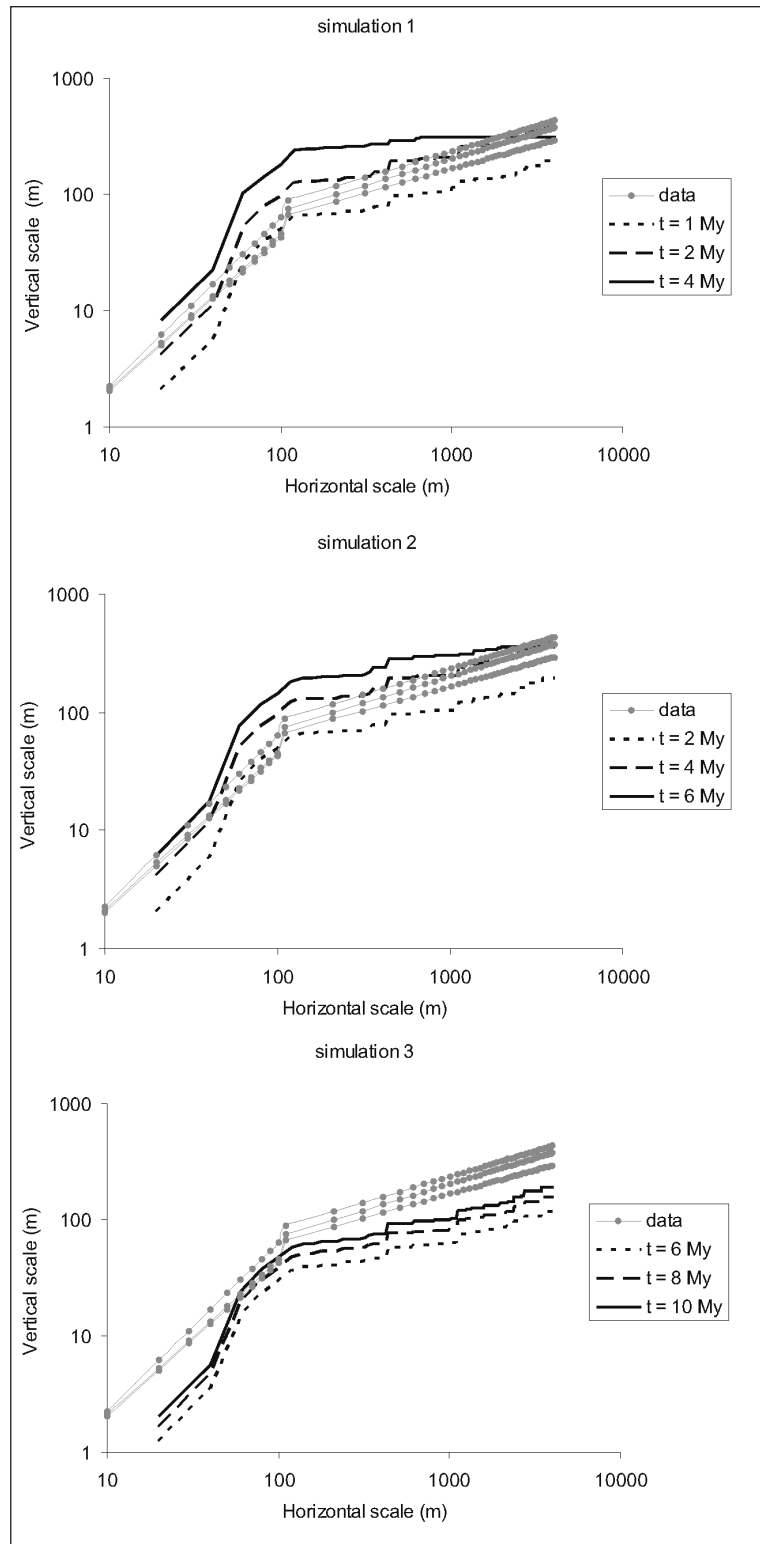
ifying different aspects of these spatial variations, and using them to refine our model if necessary.

Considering that underground dissolution has been shown to be a significant factor in the evolution of surface karst geomorphology, as highlighted in the epikarst, the simulations obtained using our model are encouraging. The spatial-anisotropic dissolution model reveals that the lowest topography locations on the hillslope receive the largest quantity of infiltrating water, and vice versa. Consequently, dissolution of the topography is more active downslope.

The aim of the present study on the morphology of cockpit karst was to simulate their evolution processes on the basis of various hypotheses on their genesis. The model was based on a spatial anisotropy of dissolution processes which has already been established as being necessary to simulate karst landscape development at the scale of individual cockpits by Fleurant *et al.* (2007). Denudation rate of the topography was linked with underground dissolution through the concept of the epikarst zone.

With regard to these results, several conclusions can be summarised as follow. Results clearly show that rainfall has to be greater than 1 m/y to simulate realistic cockpit terrains. This is in good agreement with observed data and received wisdom on climatic influence on karst topography (Sweeting, 1972). The climatic factor

$$\frac{\overline{T}_r + \overline{T}_b}{\overline{T}_r}$$



is an image of the rainfall intermittency over a geological time scale. This factor tends towards unity when rainfall frequency increases. Results of our simulations clearly show a strong impact of this factor on the shape of the obtained cockpit karst. Therefore, it seems that the morphology of cockpit karst terrains can be simulated only under conditions of heavy and very frequent rainfall over millions of year periods ( $\overline{T}_b < 9 \overline{T}_r$ ).

Fig. 10 – **Model errors.** Example of relative (black curve in %) and absolute (grey curve in m) errors between the 'best' simulated curve (Simulation 1:  $t = 1.2$  My) and data (Windsor).

Fig. 10 – **Erreurs du modèle.** Exemple des erreurs relative (courbe noire en %) et absolue (courbe grise en m) entre la meilleure des simulations (simulation 1 pour le temps  $t = 1.2$  millions d'années) et les données de terrains (Windsor).

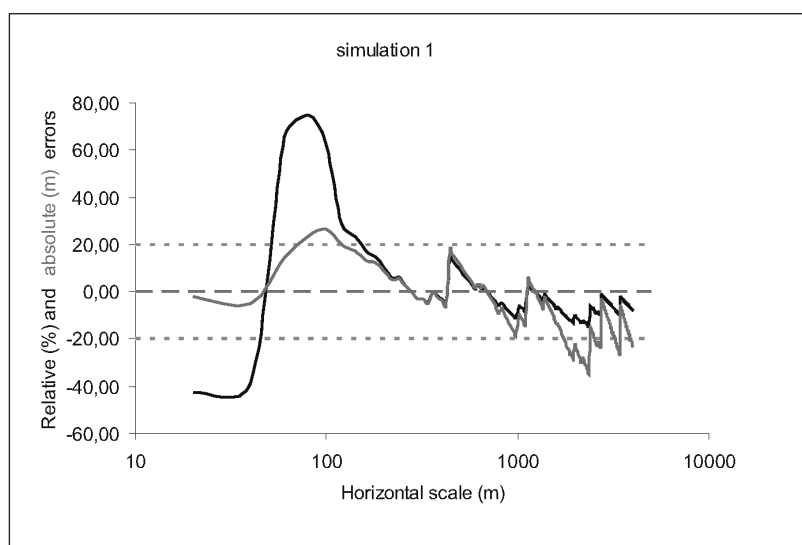
Based on the epikarst processes, and considering that the denudation rate of the surface topography is proportional to underground dissolution, we have been able to develop a cockpit karst landscape evolution model at regional scale. The model is based on a number of simplifying assumptions and could be improved in several areas if more field data become available. To compare real and simulated landscapes we have used three types of morphometric parameters: average slope, relative relief and scaling characteristics (Lyeu-Ayee, 2004). However, several other parameters could also be used to describe and compare modelled output with cockpit karst terrains and particularly geostatistic analysis or aspect analysis.

### Acknowledgments

We thank Parris Lyew-Ayee for his constructive discussions on cockpit karst country in Jamaica and three referees for their help to improve and to clarify this manuscript.

### References

- Ahnert F., Williams P.W. (1997) – Karst landform development in a three-dimensional theoretical model. *Zeitschrift für Geomorphologie N.F.*, Suppl. Bd., 108, 63-80.
- Braun J., Sambridge M. (1997) – Modelling landscape evolution on geological time scales: a new method based on irregular spatial discretization. *Basin Research* 9, 27-52.
- Brook G.A., Hanson M. (1991) – Double Fourier series analysis of cockpit and doline and karst near browns town, Jamaica. *Physical Geography* 12, 1, 37-54.
- Clemens T., Hückinghaus D., Sauter M., Liedl R., Teutsch G. (1997) – Modelling the genesis of karst aquifer systems using a coupled reactive network model. *Hard Rock Hydrosciences Proceedings of Rabat Symposium*, International Association of Hydrological Sciences Publ. S2, 241, 61-68.
- Corbel J. (1959) – Vitesse de l'érosion. *Zeitschrift für Geomorphologie* 12, 31-28.
- Coulthard T.J. (2001) – Landscape evolution models: a software review. *Hydrological Processes* 15, 1, 165-173.
- Coulthard T.J., Kirkby M.J., Macklin M.G. (1998) – Modelling the 1686 flood of Cam Gill Beck, Starbotton. upper Warfedale. In: Howard A, Macklin MG (Eds). *The Quaternary of the Eastern Yorkshire Dales*. Field Guide. Quaternary Research Association, London, 11-18.



- Densmore A.L., Ellis M.A., Anderson R.S. (1998) – Landsliding and the evolution of normal fault-bounded mountains. *Journal of Geophysical Research* 103, 15203-15219.
- Dietrich W. E., Bellugi D., Heimsath A. M., Roering J. J., Sklar L., Stock J. D. (2003) – Geomorphic transport laws for predicting the form and evolution of landscapes. In: P. Wilcock & R. Iverson (Eds) *Prediction in Geomorphology*, AGU Geophysical Monograph Series 135, 103-132.
- Dreybrodt W. (1988) – *Processes in Karst Systems*. Springer, Berlin, 452 p.
- Fleurant C, Tucker G.E. and Viles H.A. (2007) – Modèle d'évolution de paysages, application aux karsts en cockpit de Jamaïque. *Karstologia* 49, 33-42.
- Ford D.C. (1981) – Geologic Structure and a New Exploration of Limestone Cavern Genesis. *Transactions of the Cave Research Groups of Great Britain* 13, 81-94.
- Ford D.C., Williams P.W. (1989) – *Karst geomorphology and hydrology*. Unwin Hyman, London, 551 p.
- Groves C.G., Howard A.D. (1994) – Early development of karst systems 1. Preferential flow path enlargement under laminar flow. *Water Resources Research* 30, 10, 2837-2846.
- Howard A.D. (1994) – A detachment-limited model of drainage-basin evolution. *Water Resources Research* 30, 7, 2261-2285.
- Jennings J. N. (1985) – *Karst geomorphology*. Oxford, Blackwell, 510 p.
- Kaufmann G., Braun J. (1999) – Karst aquifer evolution in fractured rocks. *Water Resources Research* 35, 11, 3223-3238.
- Kaufmann G., Braun J. (2000) – Karst aquifer evolution in fractured, porous rocks. *Water Resources Research* 36, 6, 1381-1392.
- Kaufmann G., Braun J. (2001) – Modelling karst denudation on a synthetic landscape. *Terra Nova* 13, 5, 313-320.
- Lyew-Ayee P. (2004) – *Digital topographic analysis of cockpit karst: a morpho-geological study of the cockpit country region, Jamaica*. Ph.D. Thesis, University of Oxford, 210 p.
- Pfeffer K.H. (1997) – Paleoclimate and tropical karst in the west Indies. *Zeitschrift für Geomorphologie, N.F.*, Suppl. Bd., 108, 5-13.
- Singhal B., R. Gupta (1999) – *Applied Hydrogeology of Fractured Rocks*. Kulwer Academic Press, Dordrecht, The Netherlands, 400 p.

- Smith D.I., Drew D.P., Atkinson T.C. (1972)** – Hypotheses of karst landform development in Jamaica. *Transaction Cave Research Group of Great Britain* 14, 12, 159-173
- Sweeting M.M. (1972)** – *Karst Landforms*. MacMillan, London, 352 p.
- Trudgill S.T. (1985)** – *Limestone Geomorphology*. London, Longman, 196 p.
- Tucker G.E., Slingerland R.L. (1994)** – Erosional dynamics, flexural isostasy, and long-lived escarpments: a numerical modeling study. *Journal of Geophysical Research* 99, 12229-12243.
- Tucker G.E., Gasparini N., Bras R.L., Lancaster S.L. (1999)** – A 3D Computer Simulation Model of Drainage Basin and Floodplain Evolution: Theory and Applications. *Technical report prepared for U.S. Army Corps of Engineers Construction Engineering Research Laboratory*, 623 p.
- Tucker G.E., Bras R.L. (2000)** – A stochastic approach to modeling the role of rainfall variability in drainage basin evolution. *Water Resources Research* 36, 7, 1953-1964.
- Tucker G.E., Lancaster S.T., Gasparini N., Bras R.E. (2001)** – The channel-hillslope integrated landscape development model (CHILD). In: Harmon and Doe (Eds) *Landscape Erosion and Evolution Modeling*, Kluwer Publishing, Dordrecht, 349-388.
- Versteeg H.K., Malalasekera W. (1995)** – *An introduction to computational fluid dynamics: The finite volume method*. Longman, New York, 257 p.
- Weissel J.K., Pratson L.F., Malinverno A. (1994)** – The length-scaling properties of topography. *Journal of Geophysical Research* 99(B7), 13,997-14,012.
- Willgoose G.R., Bras R.L., Rodriguez-Iturbe I. (1991)** – A physically based coupled network growth and hillslope evolution model, 1, theory. *Water Resources Research* 27, 1671-1684.
- Williams P.W. (1983)** – The role of the subcutaneous zone in karst hydrology. *Journal of Hydrology* 61, 45-67.
- Williams P.W. (1985)** – Subcutaneous hydrology and the development of doline and cockpit karst. *Zeitschrift für Geomorphologie, N.F.*, 29, 4, 463-482.
- White W.B. (1984)** – Rate processes: chemical kinetics and karst landform development. In La Fleur (Eds), *Groundwater as a geomorphic agent*, Allen and Unwin, 227-248.

Article soumis le ??????, accepté le ?????? 2007.